**Supporting Information**

# Long-Range Electronic Communication in Metal-Free *meso*-Poly(Ferrocenyl)-Containing Porphyrins

Victor N. Nemykin,*[†] Gregory T. Rohde,[†] Christopher D. Barrett,[†] Ryan G. Hadt,[†] Jared R. Sabin,[†] Giacomo Reina,[†,‡] Pierluca Galloni,*[‡] Barbara Floris[‡]

**Full citation for Gaussian 03:**

**[37] M. J. Frisch, G.W. Trucks, H. B. Schlegel, G. E. Scuseria,M. A. Robb, J. R. Cheeseman, J. A. Montgomery, Jr., T. Vreven, K. N. Kudin, J. C. Burant, J.M.Millam, S. S. Iyengar, J. Tomasi, V. Barone, B. Mennucci, M. Cossi, G. Scalmani, N. Rega, G. A. Petersson, H. Nakatsuji, M. Hada, M. Ehara, K. Toyota, R. Fukuda, J. Hasegawa, M. Ishida, T. Nakajima, Y. Honda, O. Kitao, H. Nakai, M. Klene, X. Li, J. E. Knox, H. P. Hratchian, J. B. Cross, V. Bakken, C. Adamo, J. Jaramillo, R. Gomperts, R. E. Stratmann, O. Yazyev, A. J. Austin, R. Cammi, C. Pomelli, J. Ochterski, P. Y. Ayala, K. Morokuma, G. A. Voth, P. Salvador, J. J. Dannenberg, V. G. Zakrzewski, S. Dapprich, A. D. Daniels, M. C. Strain, O. Farkas, D. K. Malick, A. D. Rabuck, K. Raghavachari, J. B. Foresman, J. V. Ortiz, Q. Cui, A. G. Baboul, S. Clifford, J. Cioslowski, B. B. Stefanov,G. Liu,A. Liashenko, P. Piskorz, I. Komaromi, R. L.Martin, D. J. Fox, T. Keith, M. A. Al-Laham, C. Y. Peng, A. Nanayakkara,M. Challacombe, P.M.W. Gill, B. G. Johnson, W. Chen, M. W. Wong, C. Gonzalez and J. A. Pople, *GAUSSIAN 03 (Revision C.02)*, Gaussian, Inc., Wallingford, CT, 2004.**

**Supporting Information Table 1**. Comparison of X-ray and DFT predicted geometries in ferrocenyl-containing porphyrins.

| | $H_2$TFcP | | $H_2Fc_3PhP$ | *cis*-$H_2Fc_2Ph_2P$ | *trans*-$H_2Fc_2Ph_2P$ | $H_2FcPh_3P$ |
|---|---|---|---|---|---|---|
| | X-Ray | DFT (BPW91) | DFT (BPW91) | DFT (BPW91) | DFT (BPW91) | DFT (BPW91) |
| Bond distance (Å) | | | | | | |
| N-C(α–pyrr1) | 1.377(5) | 1.376 | 1.377 | 1.377 | 1.377 | 1.377 |
| N-C(α–pyrr2) | 1.369(5) | 1.368 | 1.367 | 1.367 | 1.368 | 1.369 |
| **average** | 1.373 | 1.372 | 1.372 | 1.372 | 1.373 | 1.373 |
| C(α–pyrr1)- C(β–pyrr1) | 1.439(5) | 1.432 | 1.433 | 1.433 | 1.434 | 1.434 |
| C(α–pyrr2)- C(β–pyrr2) | 1.445(5) | 1.457 | 1.459 | 1.459 | 1.459 | 1.460 |
| **average** | 1.442 | 1.445 | 1.446 | 1.446 | 1.447 | 1.447 |
| C(β–pyrr1)- C(β–pyrr2) | 1.358(5) | 1.363 | 1.363 | 1.362 | 1.362 | 1.362 |
| C(α–pyrr1)- C(*meso*) | 1.413(5) | 1.418 | 1.418 | 1.416 | 1.415 | 1.414 |
| C(α–pyrr2)- C(*meso*) | 1.408(5) | 1.413 | 1.411 | 1.410 | 1.410 | 1.408 |
| **average** | 1.411 | 1.416 | 1.415 | 1.413 | 1.412 | 1.411 |
| C(*meso*)- C(*ipso*-Fc) | 1.482(5) | 1.487 | 1.487 | 1.490 | 1.489 | 1.490 |
| Fe-Fe (adjacent) | 9.755 | 9.795 | 9.834, 9.793 | 9.747 | | |
| Fe-Fe (opposite) | 11.469 | 12.012 | 12.189 | | 12.636 | |
| Fe-C($Cp_1$,average) | 2.0498 | 2.059 | 2.086 | 2.085 | 2.084 | 2.085 |
| Fe-C($Cp_2$,average) | 2.0496 | 2.057 | 2.081 | 2.082 | 2.082 | 2.082 |
| Angles ($^o$) | | | | | | |
| C(α–pyrr1)-N-C(α–pyrr2) | 108.3(3) | 108.5 | 108.4 | 108.3 | 108.3 | 108.2 |
| N-C(α–pyrr1)-C(β–pyrr1) | 108.6(3) | 110.5 | 110.6 | 110.7 | 110.7 | 110.8 |
| N-C(α–pyrr2)-C(β–pyrr2) | 108.0(3) | 106.1 | 106.2 | 106.2 | 106.3 | 106.3 |
| **average** | 108.3 | 108.3 | 108.4 | 108.5 | 108.5 | 108.6 |
| N-C(α–pyrr1)-C(*meso*) | 125.5(4) | 126.1 | 126.2 | 126.4 | 126.7 | 126.7 |
| N-C(α–pyrr2)-C(*meso*) | 124.6(4) | 125.9 | 125.9 | 126.0 | 126.1 | 126.1 |
| **average** | 125.1 | 125.9 | 126.1 | 126.2 | 126.4 | 126.4 |

| Torsion angles ($^{o}$) | | | | | | |
|---|---|---|---|---|---|---|
| C(α–pyrr1)-C(*meso*)-C(*ipso*-Fc)-C(α-Cp) | 43.79 | 45.11 | 41.62 | 43.07 | 46.12 | 44.78 |
| C(α–pyrr2)-C(*meso*)-C(*ipso*-Fc)-C(α-Cp) | 42.37 | 41.77 | 43.17, 44.77 | 45.42 | 46.12 | |
| Average distortion of porphyrin core from N4 plane | | | | | | |
| | | 0.3031 | 0.2509 | 0.2037 | 0.1688 | 0.1281 |

NH protons region

(A)

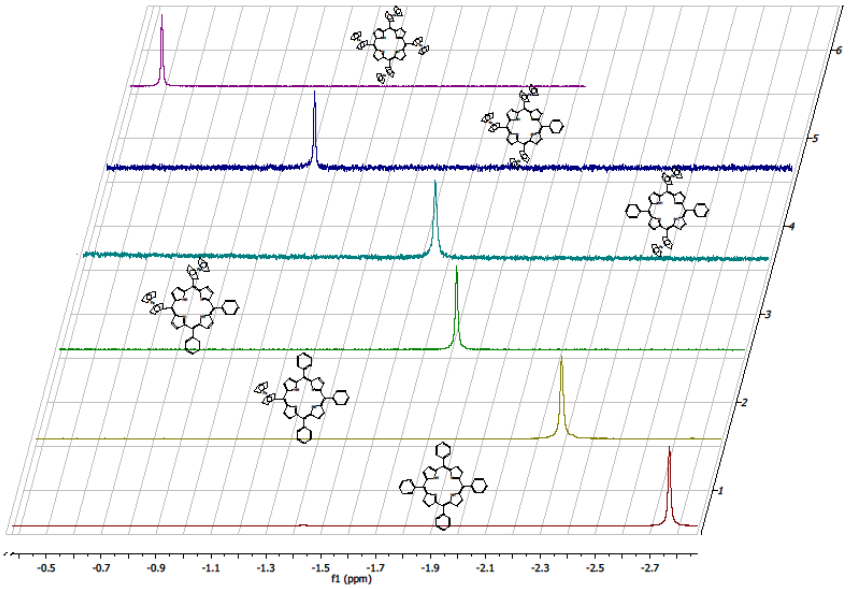


Ferrocene protons region

(B)

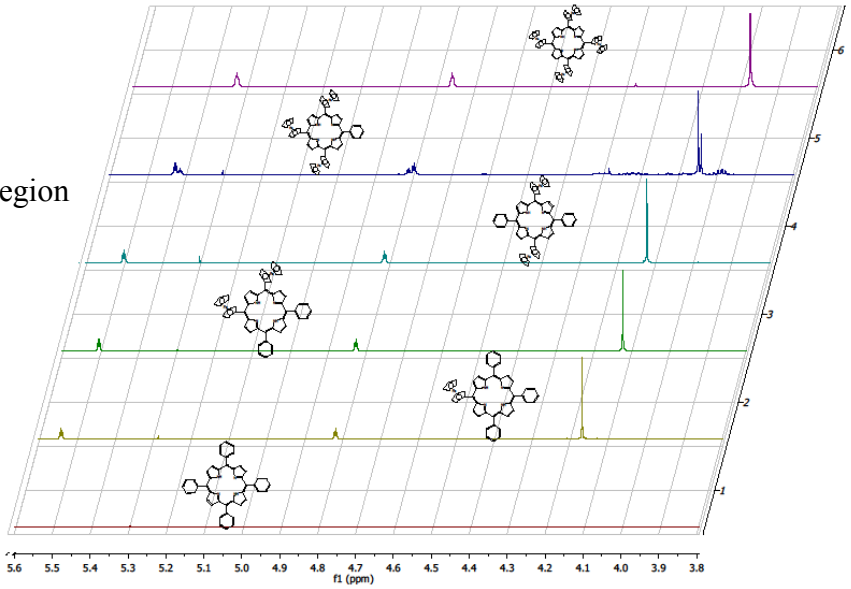


Pyrrolic and phenyl protons region

(C)

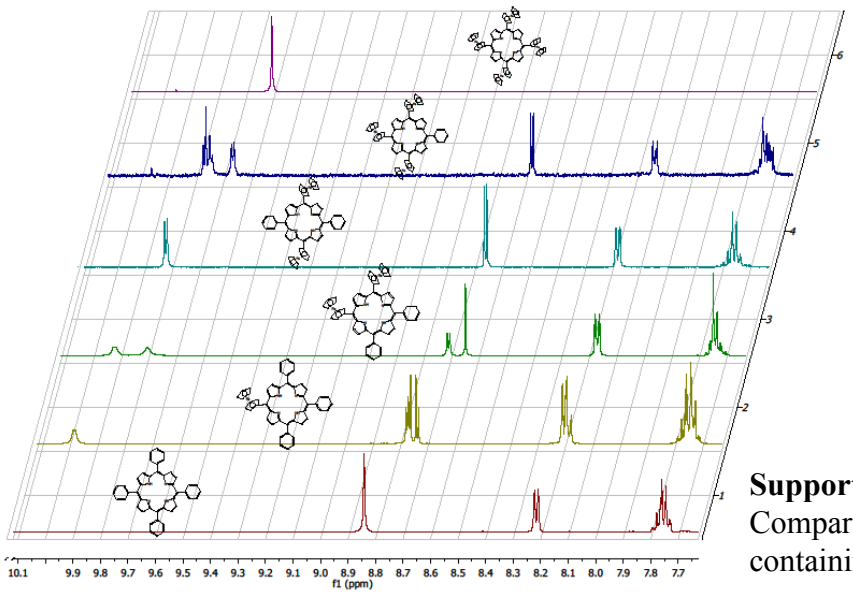


**Supporting Information Figure 1.**
Comparative $^{1}H$ NMR spectra of ferrocenyl-containing porphyrins as compared to $H_2TPP$.

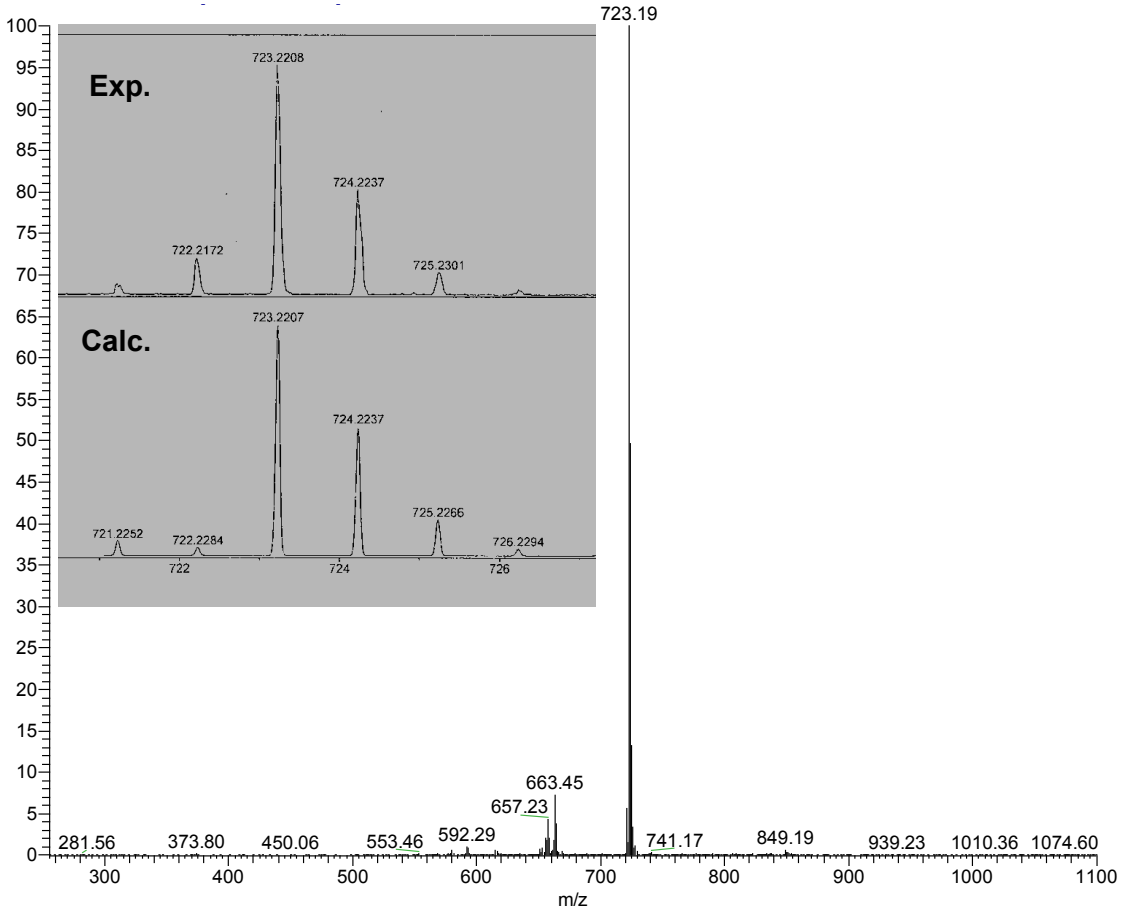


**Supporting Information Figure 2.** APCI (full view) and HS-ESI (Inset) MS of $H_2FcPh_3P$.

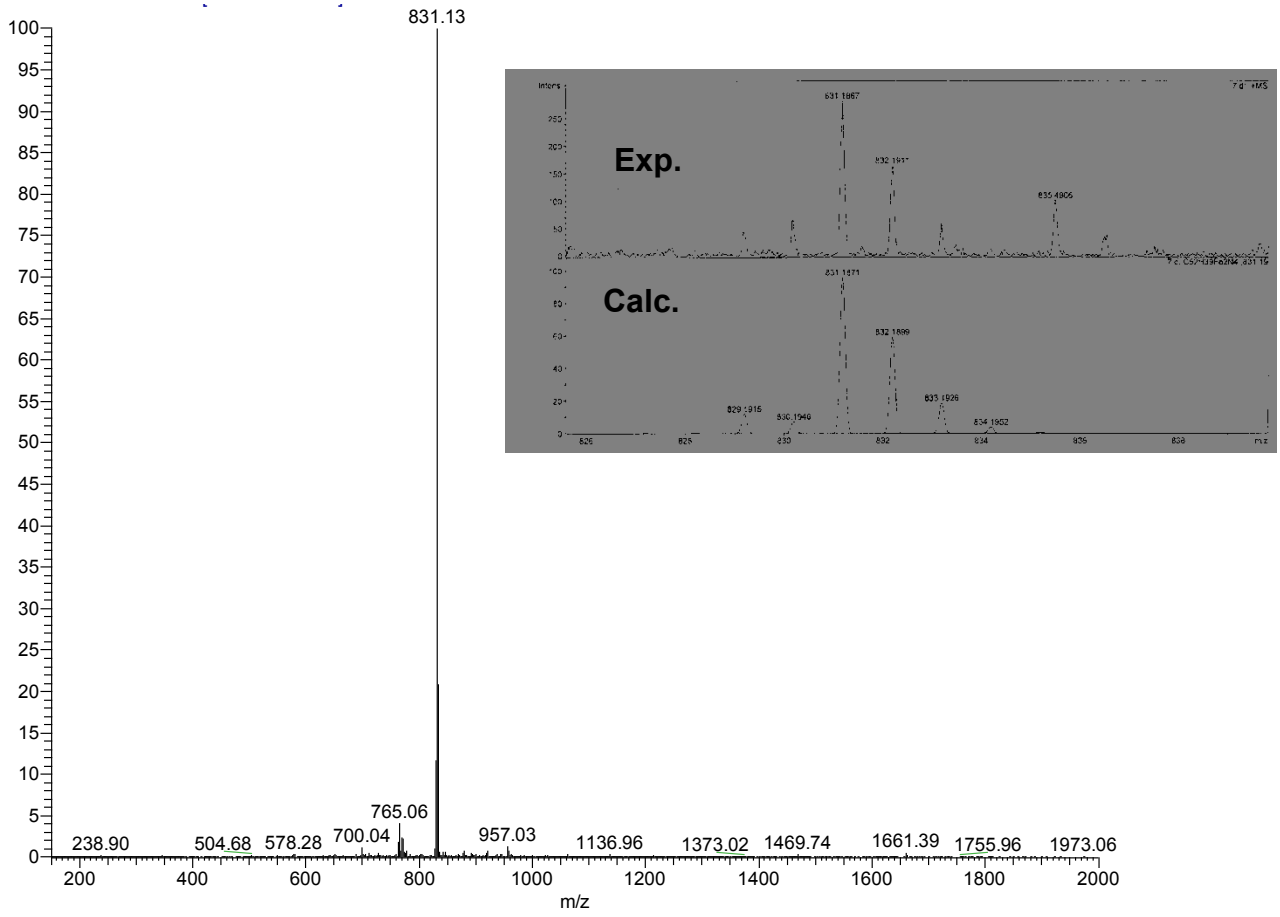


**Supporting Information Figure 2.** APCI (full view) and HS-ESI (Inset) MS of *cis*-$H_2Fc_2Ph_2P$.

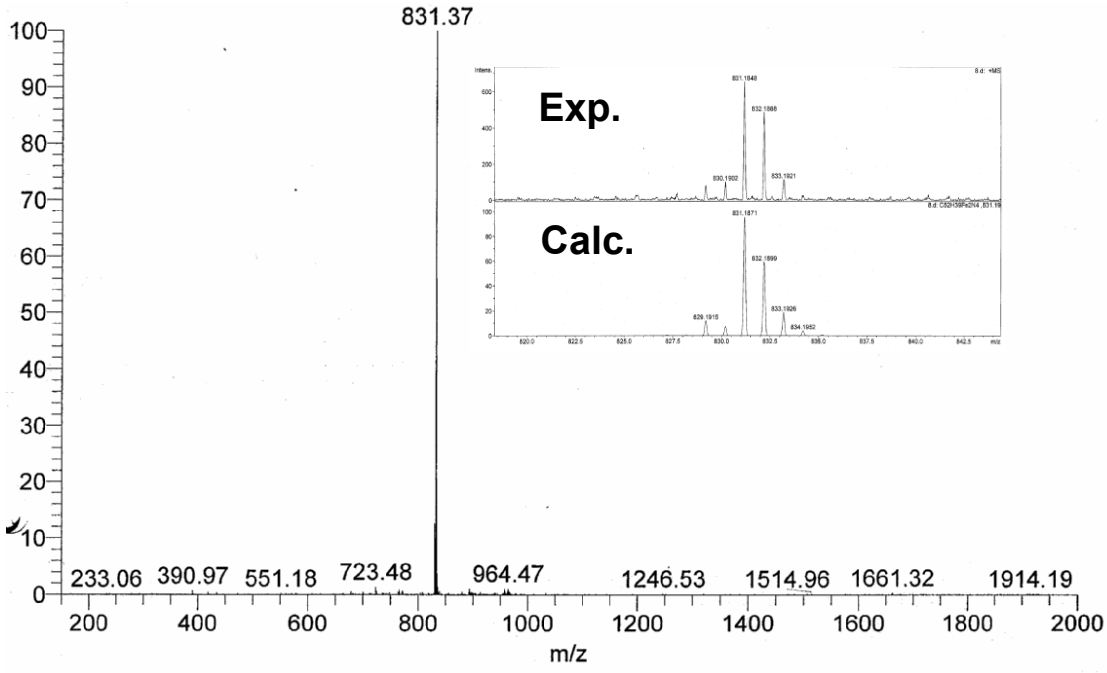


**Supporting Information Figure 2.** APCI (full view) and HS-ESI (Inset)of *trans*-$H_2Fc_2Ph_2P$

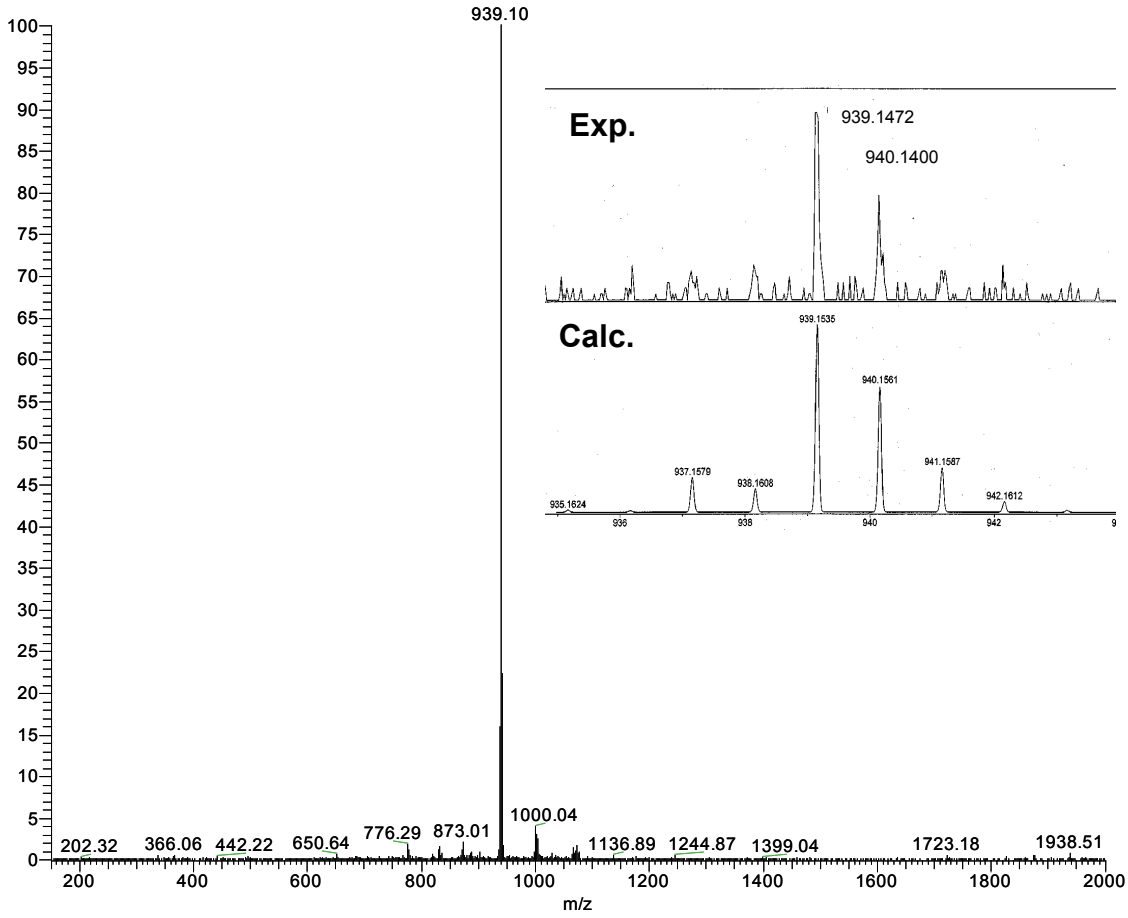


**Supporting Information Figure 2.** APCI (full view) and HS-ESI (Inset) MS of $H_2Fc_3PhP$.

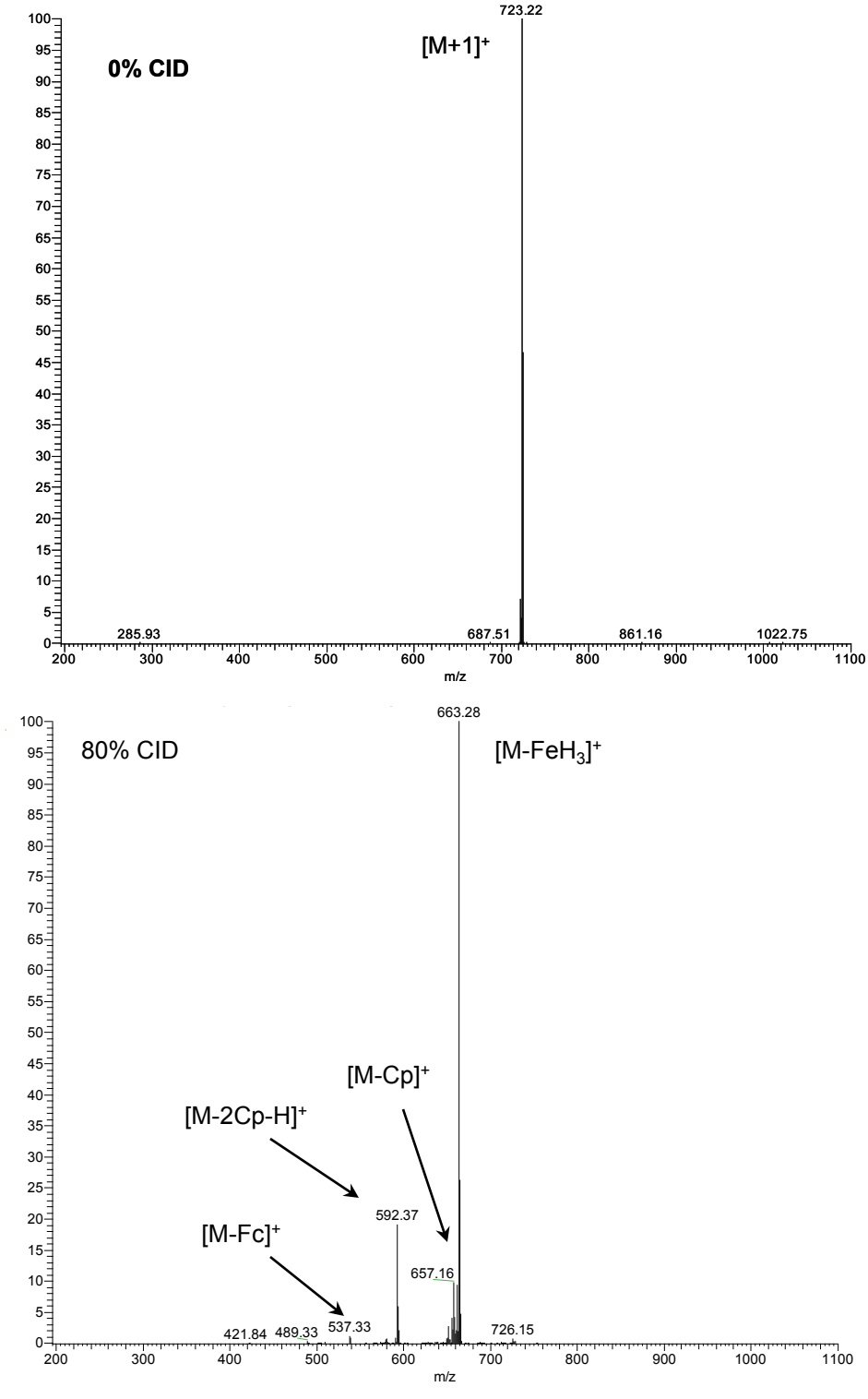


**Supporting Information Figure 2.** Partial APCI MS/MS spectra of $H_2FcPh_3P$.

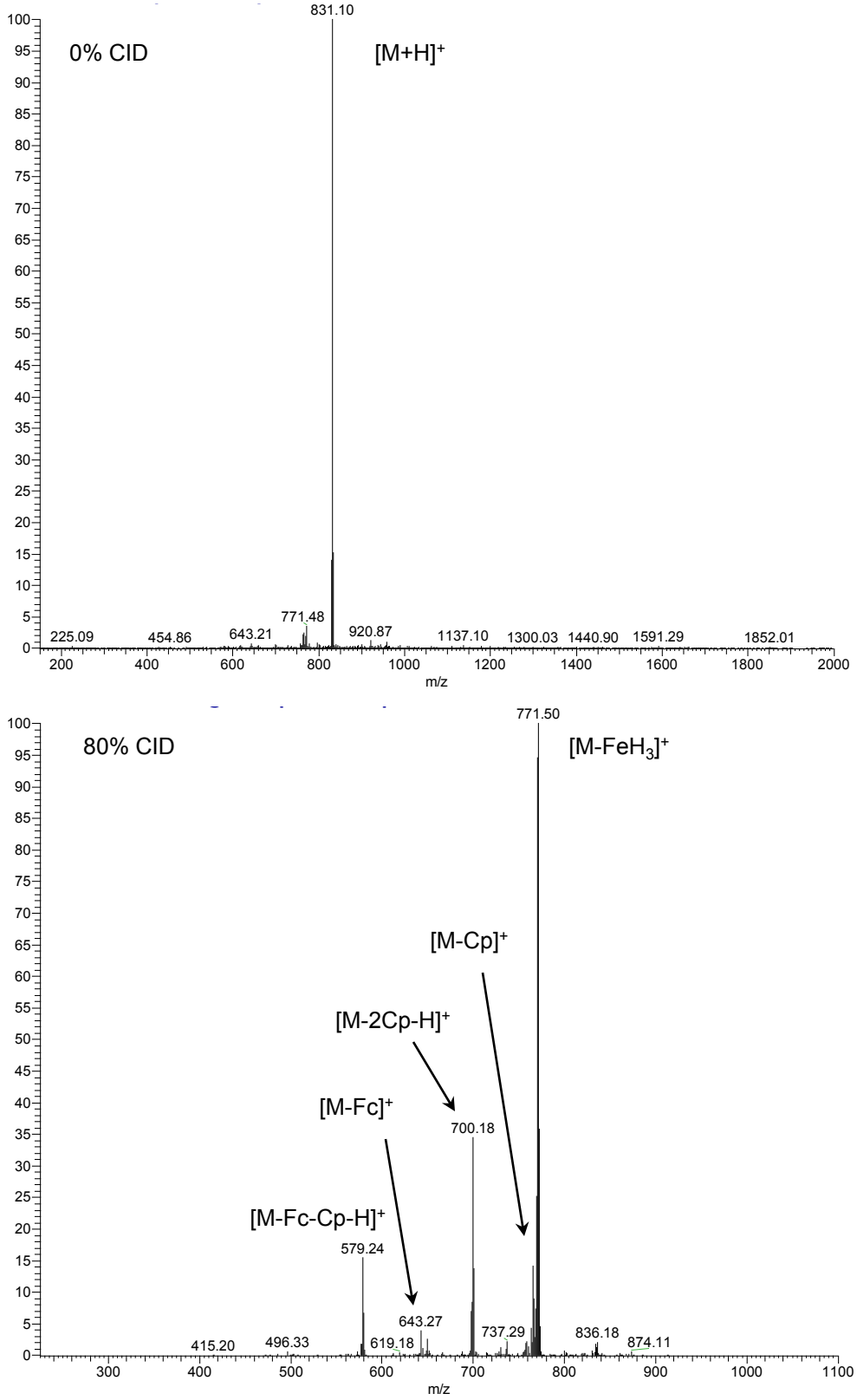


**Supporting Information Figure 2.** Partial APCI MS/MS spectra of *trans*-$H_2Fc_2Ph_2P$.

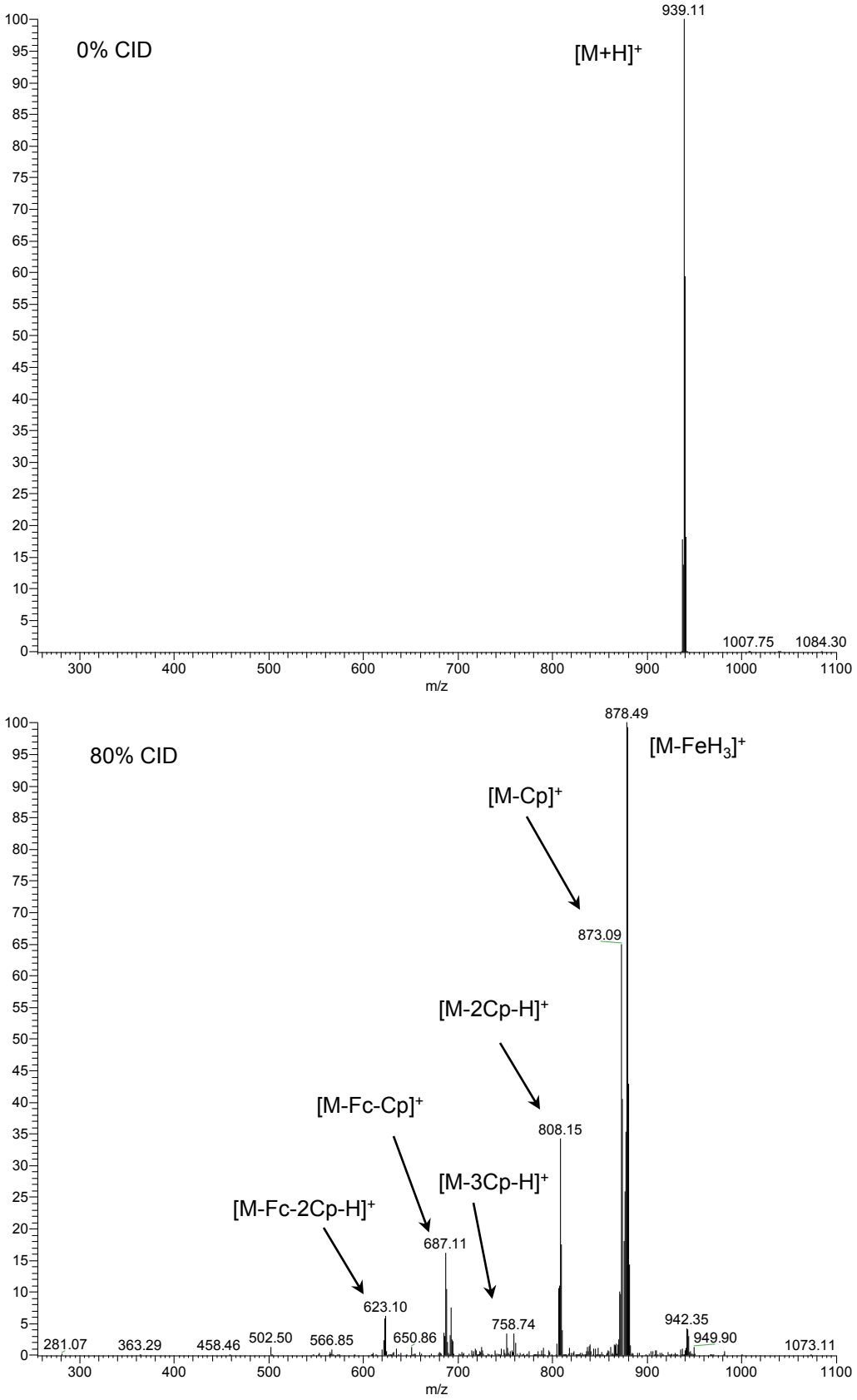


**Supporting Information Figure 2.** Partial APCI MS/MS spectra of $H_2Fc_3PhP$.

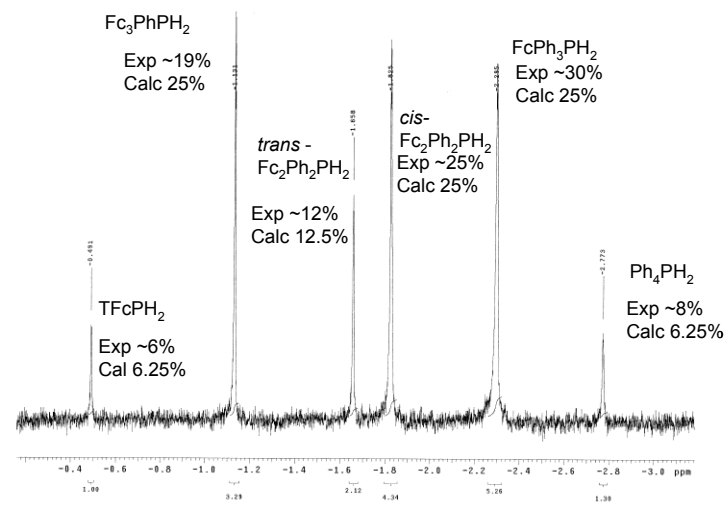


**Supporting Information Figure 3.** $^{1}$H NMR NH proton region of the reaction mixture.

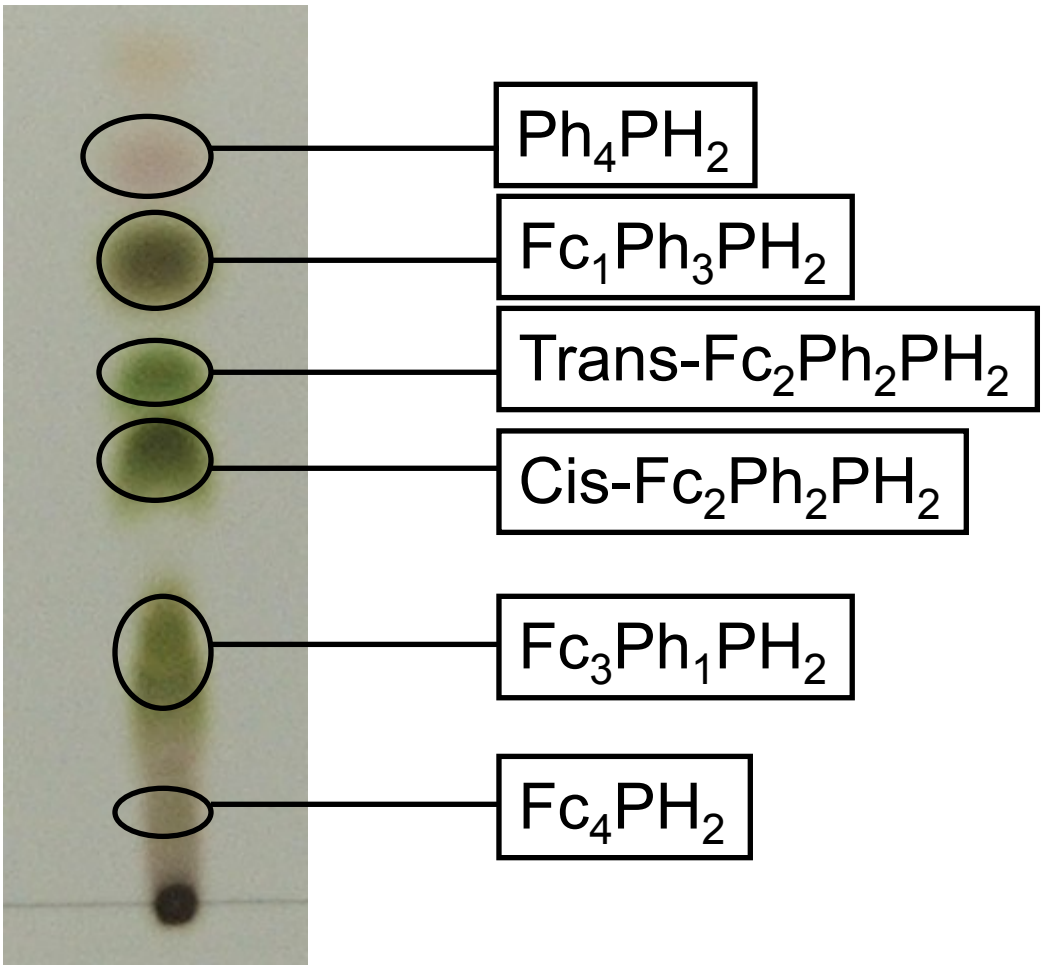


**Supporting Information Figure 4.** Separation of reaction mixture by preparative TLC.

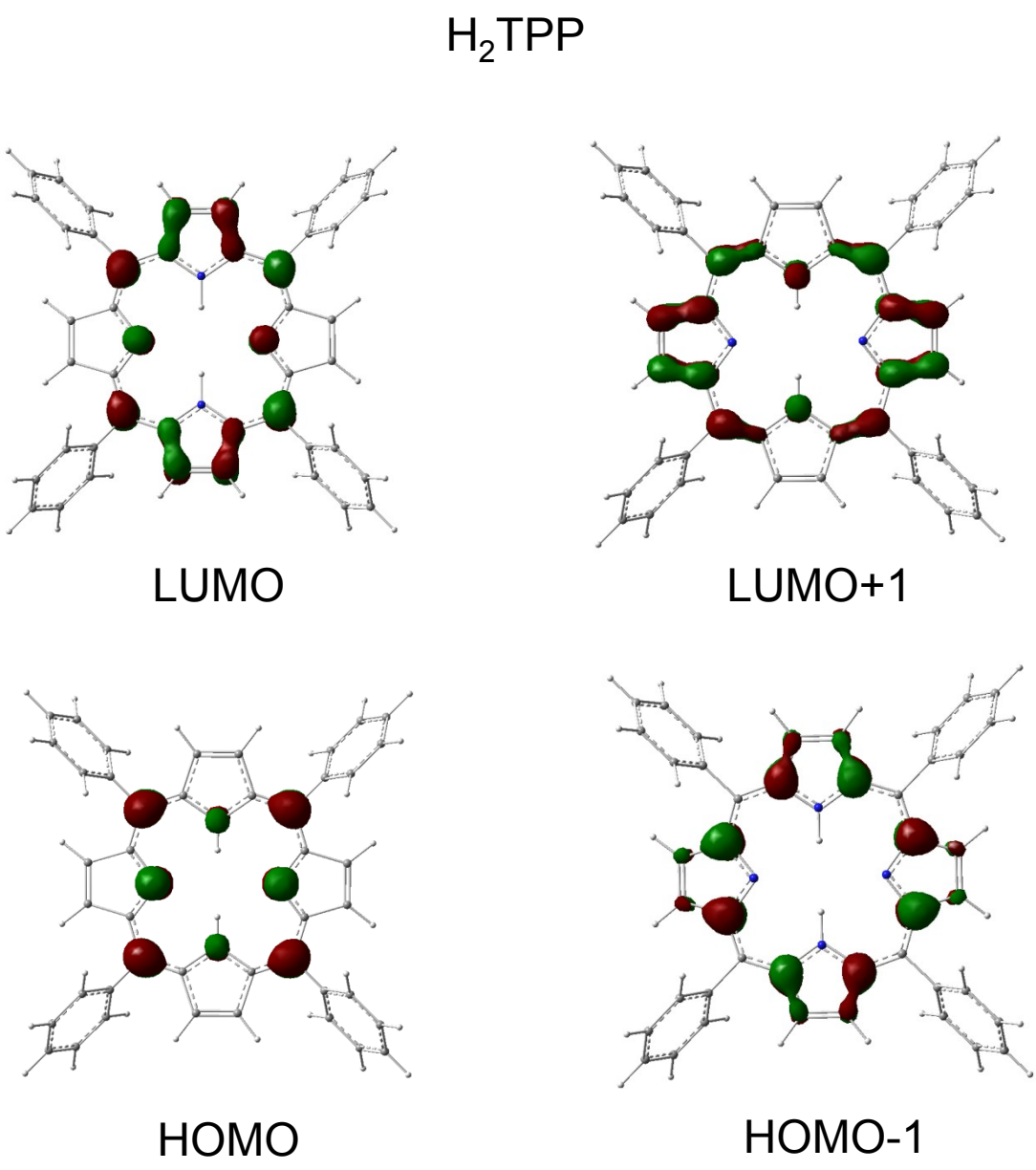


**Supporting Information Figure 5.** Important frontier orbitals calculated for ferrocenyl-containing porphyrins and $H_2TPP$.

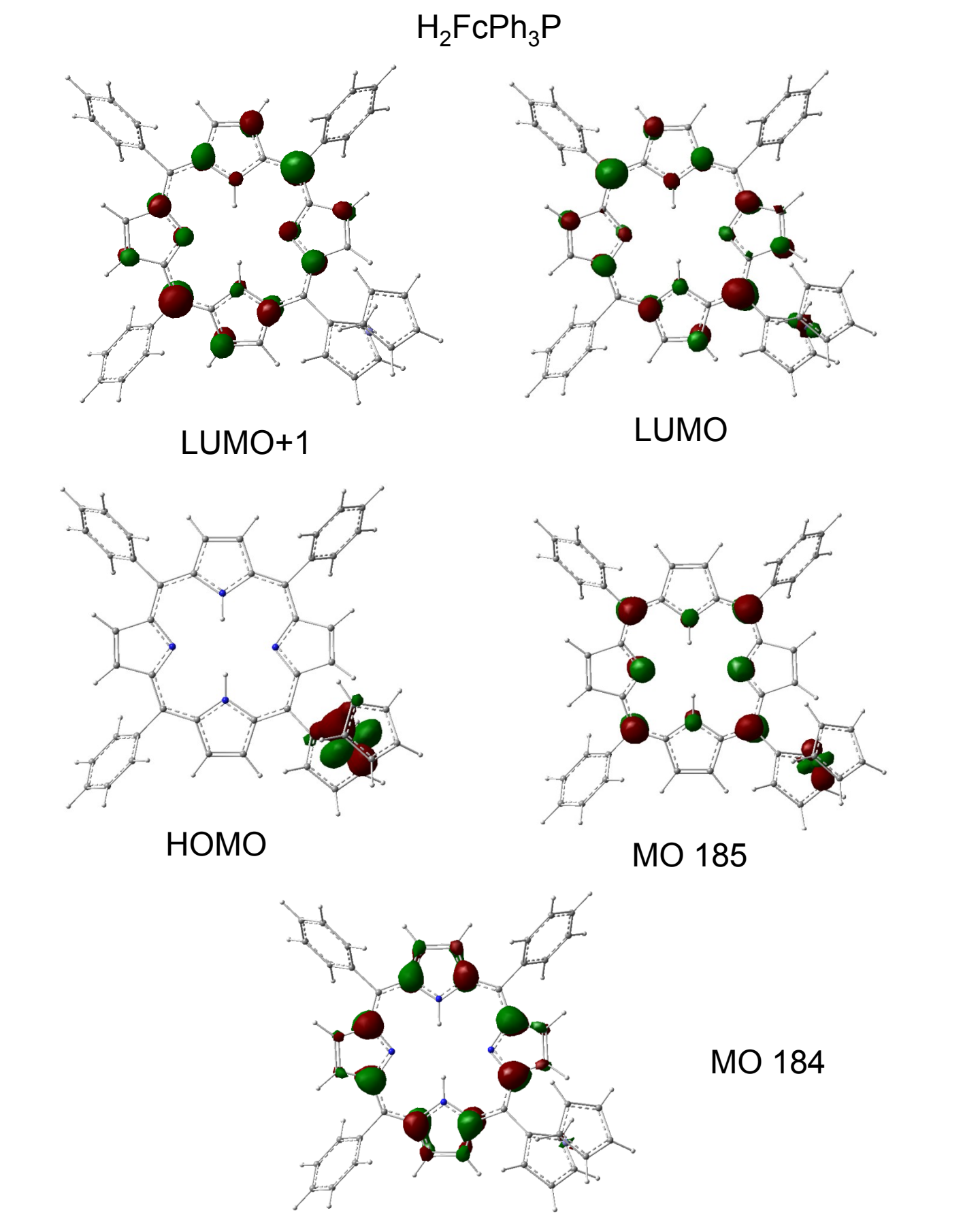


**Supporting Information Figure 5.** Important frontier orbitals calculated for ferrocenyl-containing porphyrins and $H_2$TPP.

*trans*-$H_2Fc_2Ph_2P$

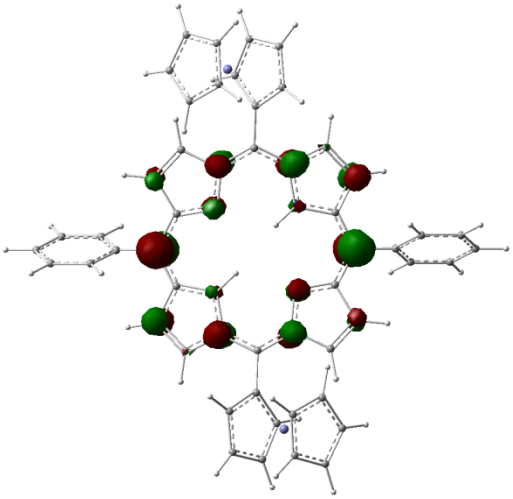

LUMO+1

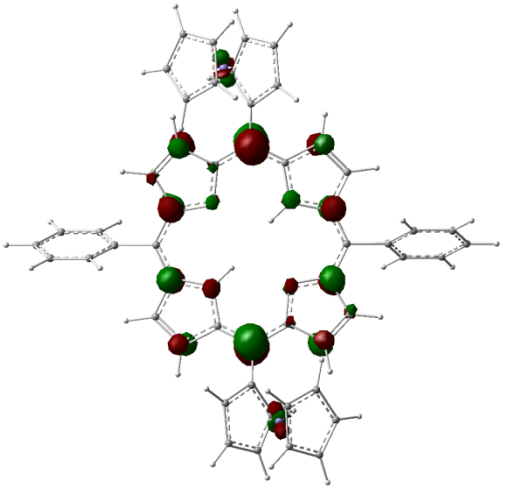

LUMO

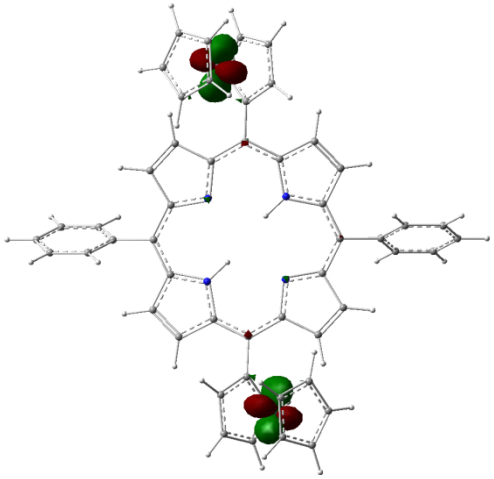

HOMO

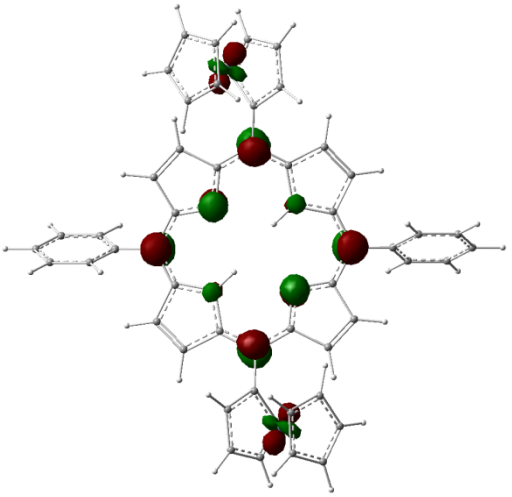

MO 209

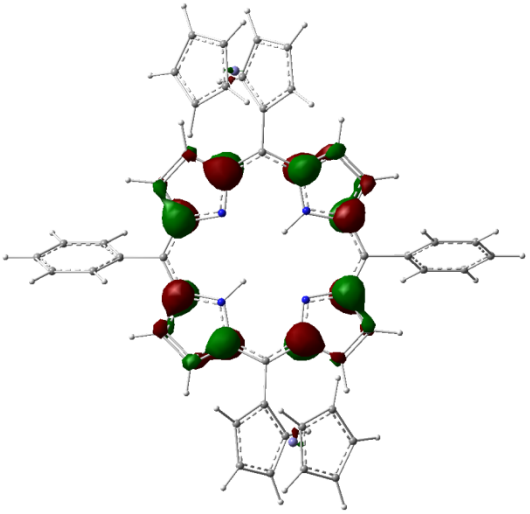

MO 208

**Supporting Information Figure 5.** Important frontier orbitals calculated for ferrocenyl-containing porphyrins and $H_2TPP$.

*cis*-$H_2Fc_2Ph_2P$

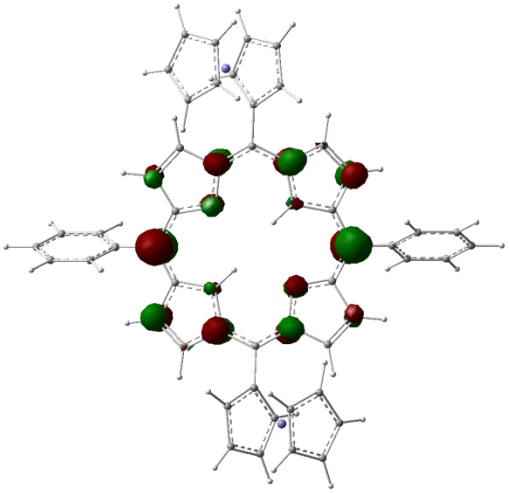

LUMO+1

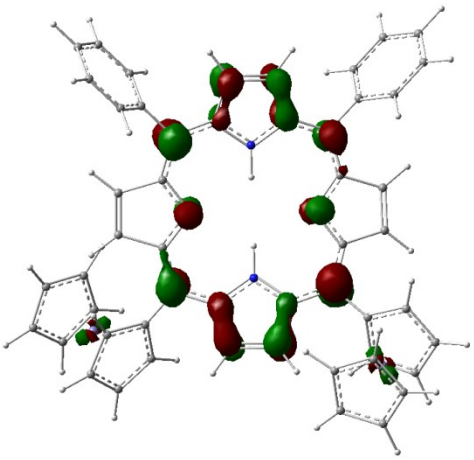

LUMO

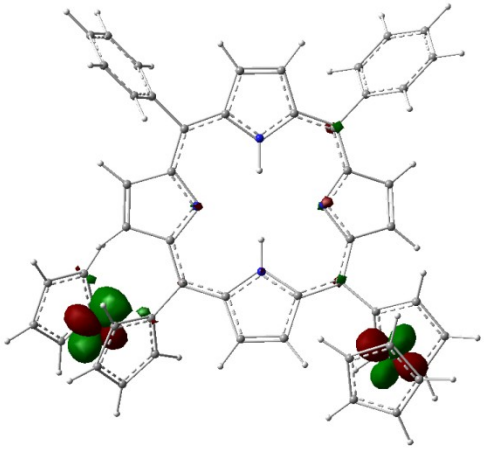

HOMO

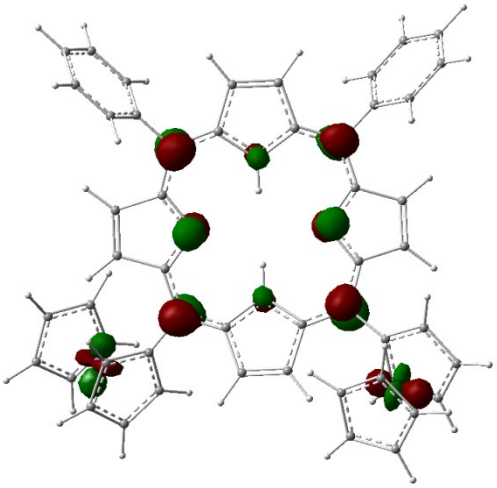

MO 209

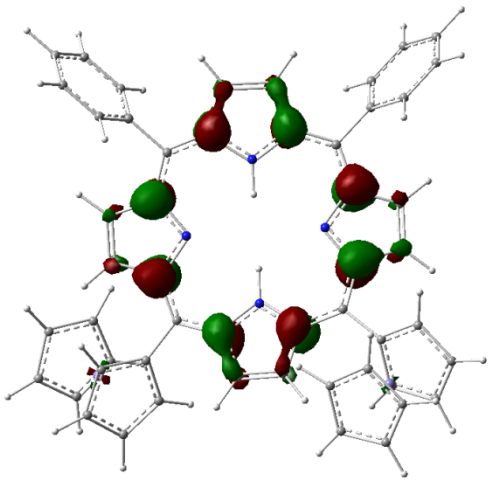

MO 208

**Supporting Information Figure 5.** Important frontier orbitals calculated for ferrocenyl-containing porphyrins and $H_2TPP$.

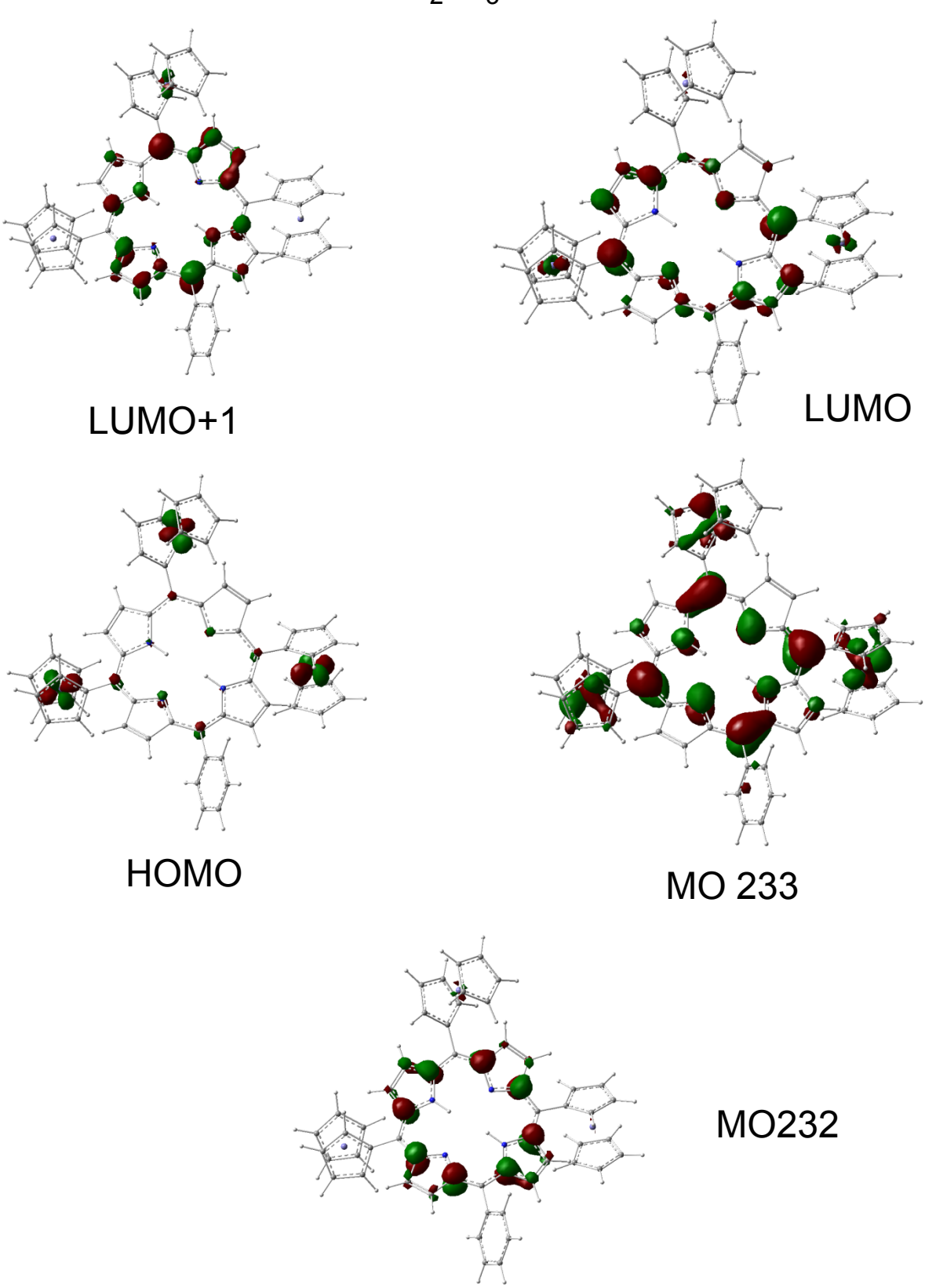


**Supporting Information Figure 5.** Important frontier orbitals calculated for ferrocenyl-containing porphyrins and $H_2TPP$.

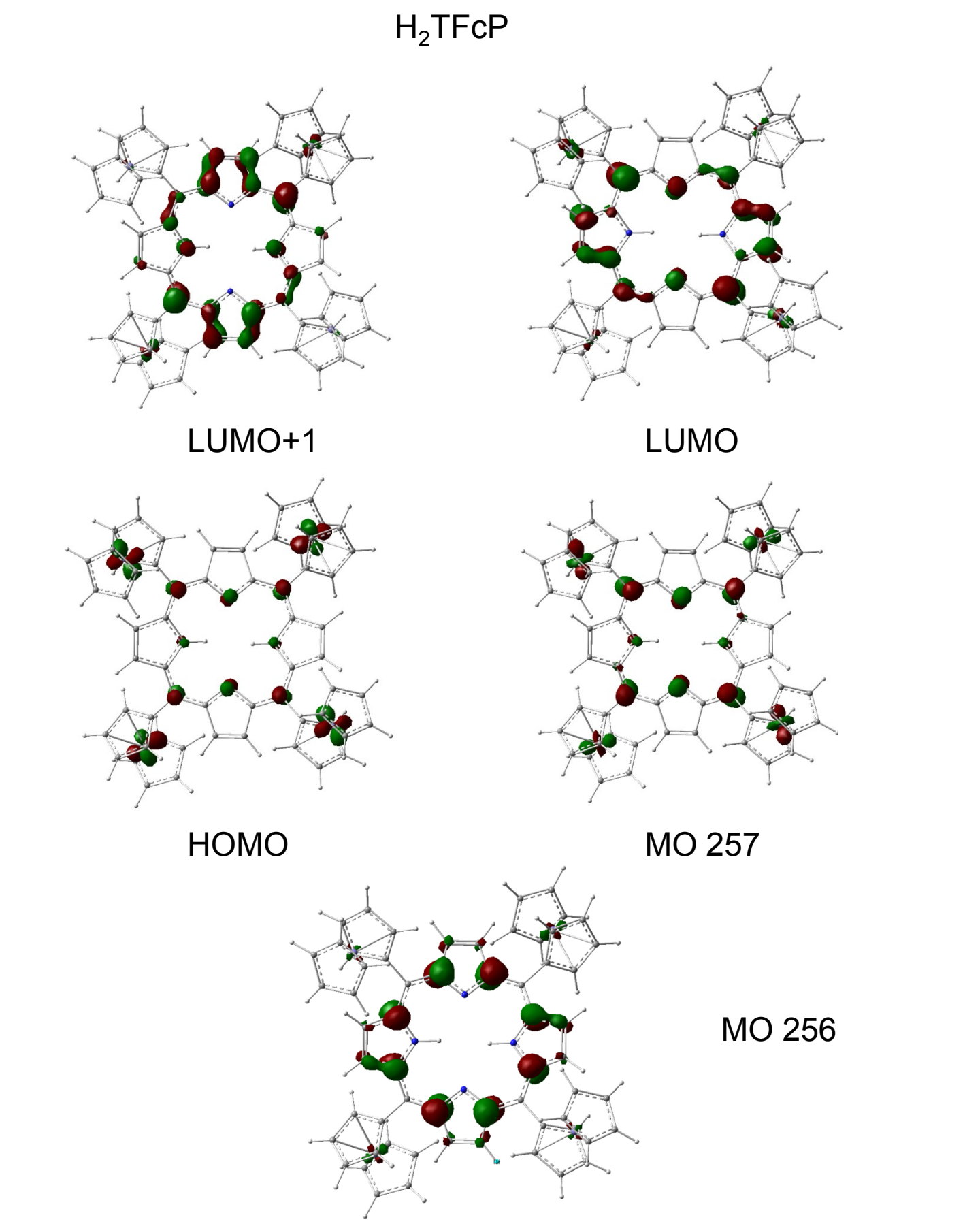


**Supporting Information Figure 5.** Important frontier orbitals calculated for ferrocenyl-containing porphyrins and $H_2TPP$.

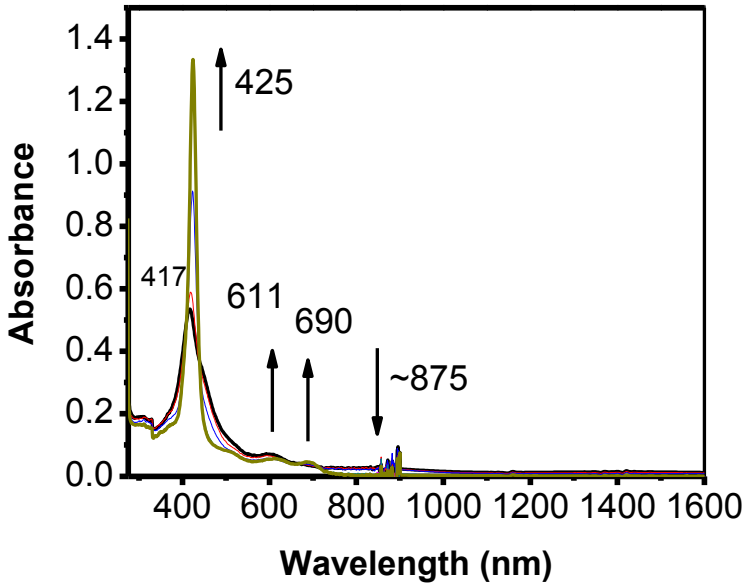


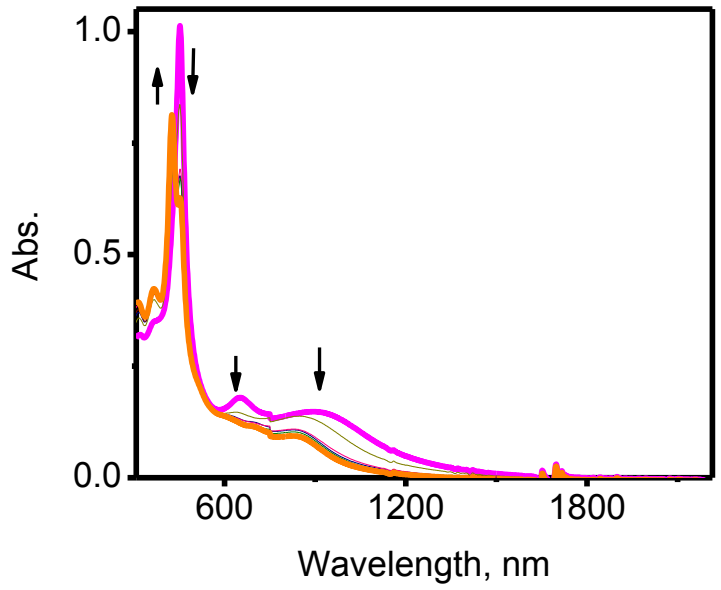


**Supporting Information Figure 6.** Reversibility of electrochemical oxidation of selected ferrocenyl-containing porphyrins. Top: reduction of *cis*-$[H_2Fc_2Ph_2P]^+$ into $H_2Fc_2Ph_2P$; bottom: reduction of $[H_2Fc_3PhP]^+$ into $H_2Fc_3PhP$.